

The Impact of Anchor Misplacement on Sensing Coverage

Yaser Al Mtawa
School of Computing,
Queen's University
Kingston, Ontario K7L 3N6
Canada
Email: yalmtawa@cs.queensu.ca

Hossam S. Hassanein
School of Computing,
Queen's University
Kingston, Ontario K7L 3N6
Canada
Email: hossam@cs.queensu.ca

Nidal Nasser
College of Engineering
Alfaisal University
Riyadh, 11533
Saudi Arabia
Email: nnasser@alfaisal.edu

Abstract—The execution of sensing services within the Internet of Things (IoT) mandates considering IoT characteristics which include heterogeneity, scalability, dynamicity, randomness, and multiple ownership. In such environment new types of sensing coverage holes posed by anchor misplacement arise. The first type is actual coverage holes that have been falsely hidden and unreported. The second one is perceived coverage holes that have been falsely generated by anchor misplacement. These types have generally been overlooked in sensing coverage research. We study these types of coverage holes in the locality of the affected sensing objects. Then we calculate the ratio of the area of each coverage holes to the total area of coverage. We utilize Delaunay Triangulation (DT) to partition the sensing region into triangles. Then we apply the concept of history in graph theory to characterize the DT structure before and after anchor misplacement. We locally detect the intra-triangle coverage hole, determine its type, and then provide the ratio of the area of this hole to the total triangle area.

Keywords— Anchor Misplacement, Wireless Sensor Network, Internet of Things, Random Deployment, Sensing Coverage, Intra-triangle Coverage, Delaunay Triangulation, History in Graph Theory.

I. INTRODUCTION

Sensing coverage measures to what extent the sensing reports reflect the true physical surroundings in the target sensing field. One of the main reasons that degrade the quality of coverage is the presence of coverage hole in WSNs. Coverage hole exists if there are some points in the sensing field are not covered by any sensing object. However, there are some applications require at least k sensing objects to cover any point in S . This type of coverage is called k -coverage and it is used to allow more fault tolerance in some critical applications such as nuclear reactor's leakage [1].

Most of the recent researches consider placement and deployment of homogeneous sensing objects for more longevity and high sensing coverage. However, recovery and detection of coverage hole attracted few works [2]. Similar to localization in WSN, the sensing coverage in WSN lacks also the global vision of IoT. For example, the current coverage schemes focus on homogeneous smart objects which belong usually to one owner (i.e. one service operator). This status shows the urgent need to tackle these issues under large scale network such as IoT.

In [3] we addressed the sensing coverage in IoT. We identified coverage holes and provided lower and upper bounds for each hole. In this paper, we will address the impact of anchor misplacement errors on sensing coverage in IoT context. Anchor misplacement problem refers to the case where an anchor is at a given position, while it reports another. Anchor misplacement

can occur due to many factors, such as errors in manual configuration, environmental factors (water current, soil erosion) and natural factors (wildlife disturbing the terrain).

In this paper we 1) formulate the problem of actual versus perceived coverage; 2) utilize Delaunay triangulation to provide theoretical analysis for the two types of coverage holes (i.e. actual unreported and false perceived coverage holes) that have been formed as a result of anchor misplacement; 3) develop an efficient algorithm to detect different types of coverage holes; 4) calculate the area ratio of each type of coverage holes to the total area; and 5) implement the algorithm and run experiments to show the correctness of our theoretical analysis. To the best of our knowledge, this is the only research that considering the impact of anchor misplacement on sensing coverage.

II. RELATED WORK AND MOTIVATION

Consider an environmental experiment to measure the air quality in a region. For this purpose, the experts use heterogeneous sensors that are already deployed in that region and belong to three different sensing providers as shown in Fig. 1. These collective shared resources will provide a better results for this experiment and, hence, improve the quality of sensing service.

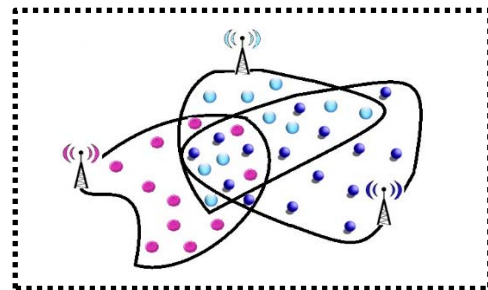


Fig. 1 Multiple sensing coverage providers.

Applications have different sensing coverage requirements [4]. For example, some applications require full sensing coverage such as applications of critical plants such as nuclear reactor. Other applications tolerate with some coverage holes such as applications in agriculture and weather forecast. Existing work on sensing coverage in WSN assume sensors are homogeneous and belong to only one sensing service provider. Most of the research addresses deterministic sensor placement and deployment planning to achieve greater coverage and/or to extend the network lifetime [5]. The sensing coverage problem is more pronounced in IoT context due to the critical challenges

of scalability, robustness, heterogeneity, and security [4] as a consequence of the explosive growth of a number of devices with different technologies being spread over a large terrain. It is predicted that IoT will consist 50 billion smart objects by 2020 [6].

Addressing WSNs in the context of IoT means that the sensing objects are: a) heterogeneous as they have different functionalities and capabilities, b) randomly deployed which is the norm in IoT, and c) belong to different sensing service providers. The challenge in such IoT setting is determining sensing coverage including the existence of coverage holes. Anchor misplacement leads to special new types of coverage holes due to inaccurate localization of some sensor nodes. The results of our previous work [7] show that anchor misplacement degrades localization accuracy. Sensing coverage quality is also affected due to: a) inaccurate data collection as the sensed data may contain inaccurate locations if their corresponding sensors were localized inaccurately using misplaced anchor nodes. This results in coverage holes and hence the full coverage is not preserved and b) inefficient energy consumption because anchor misplacement leads routing protocols to depend on inaccurate locations. Hence, drains the energy of the sensor nodes. Our previous work [3] investigates the coverage hole problem in IoT context. It identifies each coverage hole, finds its location, and calculates the lower and upper bounds of its area size. However, our previous work did not consider the existing of anchor misplacement and the new types of coverage holes that posed by this problem. In this paper, sensing coverage in the presence of anchor misplacement is addressed.

III. PRELIMINARIES

In this section, we introduce some necessary definitions and assumptions. Let S denotes the target sensing field. Let $N = \{s_i; s_i \text{ is a sensing object}; 1 \leq i \leq n\}$, be a set of sensing objects with unknown location (x_i, y_i) in a plane. Each sensor s_i has estimated location (x'_i, y'_i) and a sensing range R_{s_i} . Let p be a point in S , then p is covered if there is at least one s_i such that p is within distance of R_{s_i} from s_i . In other words, $\{\exists s_i | d(p, s_i) \leq R_{s_i}, 1 \leq i \leq n\}$, where $d(a, b)$ is the Euclidean distance between a and b .

We are interested in assessing sensing coverage and different types of coverage holes only in the locality of the anchor-misplacement-affected sensor nodes. Assume that sensor node s_i is localized by using some misplaced anchors nodes. Let $N' \subseteq N$, be the set of anchor-misplacement-affected sensor nodes or affected sensor nodes, for simplicity. We use the usual cardinality notation $|\cdot|$ to denote the size of the set. For example, $|N'|$ is the cardinality of N' . Further let C_{s_i} denotes the *actual* sensing coverage area that is covered by sensor s_i .

Definition 1: The *actual* collective sensing coverage (C_{act}) of all affected sensor nodes in WSN is defined as the union of their physical sensing coverage in the network. That is $C_{act} = \bigcup_{i=1}^{|N'|} C_{s_i}$.

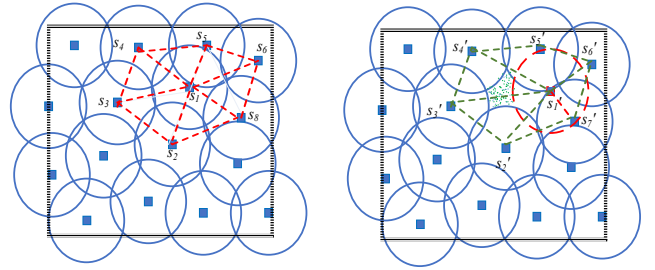
Let s'_i be the erroneous estimated location of s_i . This means that s_i will report sensed data from inaccurate location and this creates a *perceived* coverage around s'_i . Further, let C'_{s_i} denotes

the *perceived* sensing coverage area that is covered by affected sensor node s_i as if s_i in its estimated position.

Definition 2: The *perceived* collective sensing coverage (C_{per}) of all affected sensor nodes in WSN is defined as the union of their *perceived* sensing coverage in the network. That is $C_{per} = \bigcup_{i=1}^{|N'|} C'_{s_i}$.

Clearly the larger the intersection between C_{act} and C_{per} , the less perceived coverage exists and, hence, the less impact of anchor misplacement on sensing coverage. The comparison between C_{act} and C_{per} shows new types of coverage holes:

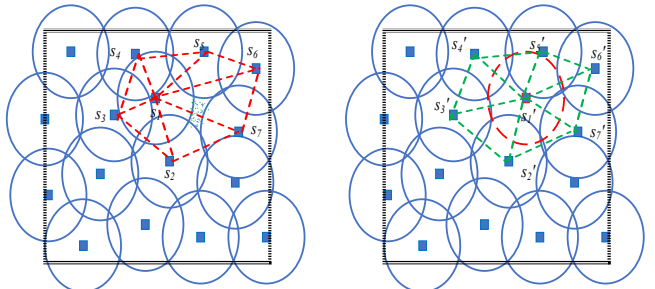
- 1) Perceived coverage hole where an area is covered actually by C_{s_i} as in Fig. 2(a), but not covered by C'_{s_i} as in Fig. 2 (b) where the hole exists in two triangles $s_1's_2's_3'$ and $s_1's_3's_4'$. In this case, $C_{act} > C_{per}$.



(a) An ideal case where no coverage holes.
(b) Perceived coverage hole due to anchor misplacement.

Fig. 2 Perceived hole can be identified by triangulation in the vicinity of the affected sensor s_1 .

- 2) Unreported actual coverage hole where an area is not covered by C_{s_i} as in Fig. 3(a) where the hole exists in triangles $s_1s_6s_7$ and $s_1s_7s_2$, but covered by C'_{s_i} as in Fig. 3(b). In this case, $C_{act} < C_{per}$.



(a) Original deployment with actual coverage hole.
(b) Actual coverage hole is masked. Thus unreported.

Fig. 3 Actual unreported can be identified by investigating the triangles in the vicinity of the affected sensor s_1 .

In practise, in order to do such comparison between C_{s_i} and C'_{s_i} and to characterize which scenarios lead to each type of sensing coverage holes, we need a computational structure that enable us to do the required calculations efficiently. For this purpose, we use Delaunay triangulation to study this problem in the locality of each affected sensor node.

IV. PROBLEM DESCRIPTION

In WSNs, sensor density must be above a specific threshold to maintain coverage; otherwise, coverage holes exist. Anchor misplacement may lead to special types of coverage holes due to inaccurate localization of the affected sensor nodes. Anchor misplacement error refers to the case where an anchor is at a given position, while it reports another. The results of our previous research [7] show that anchor misplacement degrades localization accuracy. Coverage quality is also affected due to the inaccurate data collection of the affected sensor nodes as they report sensed data from erroneous estimated locations. This results in special types of coverage holes: Actual-unreported, and false perceived coverage holes. In this paper, we address the impact of anchor misplacement on sensing coverage. Given a random deployment of sensor nodes and a localization error posed by some anchor misplacement on some sensor nodes, we are interested mainly to investigate the new types of coverage holes, and find the size ratio of each type of coverage hole to the total area.

A. Assumptions

The main assumptions in this paper are the following:

1. WSN is connected. This means that every object is able to receive and send packets to and from any other object. This assumption is important to exchange the information locally through multi-hop in order to build our computational structure in a distributed manner.
2. Localization of sensing objects is multi-iteration-based with MMSE for fine-tuning the estimated positions.
3. In order to show its impact on coverage, we assume that anchor misplacement is the most critical source of error that leads to localization uncertainty (i.e. neglect other sources of error).
4. The sensing target field is bounded. This helps constructing DT in a simpler manner.

B. Network and Sensing Models

We adopt the same network and sensing models as in [3]. That is, the random deployment for network model and binary disk as a sensing model. Random deployment refers to the case where each IoT object is deployed uniformly over the target field and independently from all other objects. On the other hand, binary disk model assumes that a point in a sensing field S is covered if it is within the sensing range of at least one sensor. Otherwise, it is not covered.

V. TOWARDS EFFICIENT SENSING COVERAGE : DELAUNAY TRIANGULATION

The problem to study the coverage problem in a sensing field S is reduced, by using Delaunay Triangulation (DT), to study the intra-triangle coverage for each triangle in DT [3]. The following Lemma characterize the full sensing coverage for each triangle Δ in DT.

Lemma 1 [3]:

A triangle Δ with is fully covered if every pair s_i and s_j of its set of vertices satisfies the following condition:

$$2r \leq R_{s_i} + R_{s_j}.$$

Let s_i be a sensor node vertex in a triangle Δ . Then s_i contributes to the intra-triangle sensing coverage of Δ . The coverage contribution of s_i is the size of the angular sector centered at s_i with radius R_s . The calculation of the contribution of s_i in Δ requires the angle at s_i . Since the lengths of all edges of Δ are known, we use the cosine formula to extract the angle at each sensor node. That is, $\alpha = \cos^{-1}\left(\frac{a^2+b^2-c^2}{2ab}\right)$, where α is the angle opposite to side of length c . Therefore, the coverage contribution of sensor s_i is $CNT(s_i, \Delta) = \frac{\alpha}{2} R_s^2$ where α is the angle at s_i in triangle Δ . Adding up the sensing coverage contributions of the three sensor nodes of Δ gives the intra-triangle coverage of Δ , denoted by $ITC(\Delta)$. That is, $ITC(\Delta) = \sum_{s_i \in V(\Delta)} CNT(s_i, \Delta)$, where $V(\Delta)$ is the set of three vertices of Δ .

VI. THE IMPACT OF ANCHOR MISPLACEMENT ON SENSING COVERAGE

Assume that some anchor nodes are randomly misplaced in sensing field S . These misplaced anchor nodes pose localization error on some sensor nodes. We use the implementation of a distributed algorithm in [8] to construct the DT that represents the target sensing field S . Lemma 1 shows that if $(R_{s_i} + R_{s_j})$ is less than the radii r of the circumcircles (circumradii) of one triangle Δ in DT, or equivalently $(R_{s_i} + R_{s_j})$ is less than the Euclidean distance between the vertices s_i and s_j , then there is a hole coverage. The uncovered area inside Δ can be calculated by subtracting the intra-triangle coverage (ITC) of Δ from the full area size of Δ . That is $A_\Delta - ITC(\Delta)$. The area size of Δ can be calculated by the following formula:

$$A_\Delta = \sqrt{d(d-a)(d-b)(d-c)}, \text{ where } d = \frac{a+b+c}{2} \text{ and } a, b \text{ and } c \text{ are the length of the sides of } \Delta.$$

Assume that one sensor node say s_2 in Fig. 4 was localized by some misplaced anchor nodes. Let $s_2'(x', y')$ be the erroneous location before any correction. Further, let $\vec{v} = (\Delta x, \Delta y)$ be the localization error vector. Then the coordinates of the corrected position for s_2 is $(x' - \Delta x, y' - \Delta y)$.

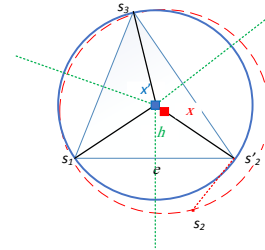


Fig. 4 An example of structural change on DT due to correcting the location of s_2' to s_2 .

In order to measure the sensing coverage holes posed by anchor misplacement, we need to calculate the sensing coverage in two cases: with and without the existence of anchor misplacement. That is, for each affected sensor node s_i , we measure the coverage hole by comparing the sensing coverage of s_i and its neighbours from one hand, and s_i' and its

neighbours on the other hand. This means we are interested to compare C_{s_i} and C'_{s_i} in their vicinities. In Fig. 2 and 3, the vicinity of affected sensor s_1 is $s_2s_3s_4s_5s_6s_7$ and the vicinity of s_1' is $s_2's_3's_4's_5's_6's_7'$. The triangulation of these vicinities enable us to study the coverage holes in each triangle.

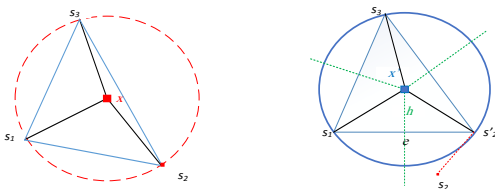
Next, we introduce a concept of history to demonstrate the above description of calculating the sensing coverage for each affected sensor node with and without anchor misplacement.

A. Anchor Misplacement as a Graph Operator

Let DT be a Delaunay Triangulation of IoT objects in the terrain. Some of these objects have known locations (i.e. anchors) and the rest have initially unknown locations. The displacement vectors of the misplaced anchor objects B_j trigger a change in DT as they impact the localization accuracy of the sensing objects. The change in DT could be in the distance metric of edges or in the structure as some objects become connected or disconnected. Let us call the new triangulation DT' . Thus anchor misplacement work as an operator which maps a given graph (i.e. DT) into a new graph DT' . Furthermore, let $NH(a)$ denotes the set of sensing objects in which each object has a common triangle edge with sensing object a . We introduce the concept of history to approach the Delaunay triangulation structure before and after anchor misplacement. The triangulation of s_1' and its vicinity (i.e. $NH(s_1') = \{s_2', s_3', s_4', s_5', s_6', s_7'\}$ in Fig. 2 and 3 represents the history of the triangulation of s_1 and its vicinity. The following is the formal definition of the history of a vertex in DT as follows.

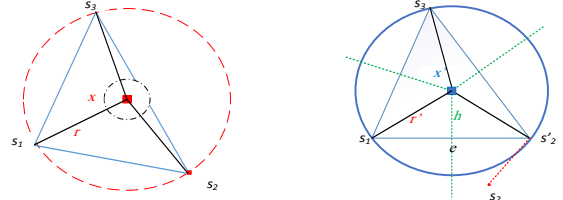
Definition 3: Let $T(s_i)$ denotes a triangulation in DT' that is induced by both s_i' and $NH(s_i')$. That is, the Delaunay triangles that have s_i' as a common vertex. Similarly, we call $T^{-1}(s_i)$ the history of a vertex s_i' and it denotes a triangulation in DT that is induced by both s_i and $NH(s_i)$, where s_i is the correct position of s_i' .

Fig. 5 shows one triangle of $T(s_2)$ and its history. The concept of history is not new in graph theory and has been used to study the asymptotic characteristics of iterated graphs such as line and path graphs [9], [10]. We note that the locations of all vertices in $T(s_i)$ are localized with the presence of anchor misplacement. However, the locations in $T^{-1}(s_i)$ are corrected as if there is no anchor misplacement or the misplacement has been reversed. Clearly the subgraphs $T(s_i)$ and $T^{-1}(s_i)$ may not be the same as some vertices can be in $T(s_i)$ but not in $T^{-1}(s_i)$ or vice versa. The location of each object in the terrain is a key point in our study as both subgraphs $T(s_i)$ and $T^{-1}(s_i)$ maybe isomorphic¹ but yet different in terms of edge lengths.



(a) One triangle of $T^{-1}(s_2)$ (b) The triangle in $T(s_2)$
Fig. 5 A partial snapshot of $T(s_2)$ and its history.

We can construct DT from DT' in the following way: Identify the misplaced anchor objects by using the algorithm in [7]. Then remove the displacement-affected objects s_i with their linked edges, and insert objects s_i again in their correct positions. Lastly, construct the triangulation in their locality. Let $\deg(s_i, G)$ denotes the number of direct neighbouring objects of object s_i in graph G . That is, $\deg(s_i, G) = |NH(s_i)|$. The average $\deg(s_i, DT)$ is at most 6 and, therefore, the average number of triangles in both subgraphs $T(s_i)$ and $T^{-1}(s_i)$ will not exceed 6 [11].



(a) Coverage hole in $T^{-1}(s_2)$ (b) The hole is masked in $T(s_2)$
Fig. 6 Unreported coverage hole with center x .

B. Coverage Holes with Anchor Misplacement

In order to study the impact of anchor misplacement on sensing coverage and detect the false coverage and actual coverage holes we are interested in the common triangles of both subgraphs, that is the triangles in $T(s_i) \cap T^{-1}(s_i)$. The empty intersection indicates that $T^{-1}(s_i)$ is totally new structure and none of $NH(s_i)$ in $T(s_i)$ is triangulated with s_i' . This happens when the error posed by anchor misplacement on localizing s_i is extremely high such that the estimated location s_i' is out of the vicinity of s_i . Any common triangle Δ in $T(s_i)$ and $T^{-1}(s_i)$ falls in one of the following categories:

- 1) The local full coverage of Δ is maintained in both $T(s_i)$ and $T^{-1}(s_i)$.
- 2) The local full coverage of Δ exists in $T^{-1}(s_i)$, but not in $T(s_i)$ (i.e. perceived coverage hole).
- 3) There is no local coverage in both $T(s_i)$ and $T^{-1}(s_i)$.
- 4) The local full coverage of Δ exists in $T(s_i)$, but not in $T^{-1}(s_i)$ (i.e. actual unreported coverage hole as in Fig.6).

Categories 1 and 3 deal with extreme cases where triangle Δ is either covered in both $T(s_i)$ and its history or not. Category 2 shows the case of perceived unreal coverage hole as Δ is not covered in $T(s_i)$, but is covered in its history. In contrary of category 2, category 4 demonstrates the actual unreported coverage hole.

The two types of coverage holes (i.e. perceived, and actual unreported coverage holes) can be identified by applying the same strategy followed in our previous work [3]. Lemma 1 is applied on each triangle Δ in $T(s_i) \cap T^{-1}(s_i)$. Once for $T(s_i)$ and another time for $T^{-1}(s_i)$. Thus, the coverage hole in Δ is identified according to the above categories. Finding C_{s_i} and C'_{s_i} in their vicinities requires the calculation of the size of coverage hole for each Δ in $T(s_i) \cap T^{-1}(s_i)$. For more readability of this analysis, let Δ' and Δ denote the same triangle (i.e. have same vertices) in $T(s_i)$ and $T^{-1}(s_i)$, respectively.

¹ Two graphs are isomorphic if they contain the same objects (i.e. vertices) linked in the same way.

The coverage ratio in category 1, RC1, can be written as a ratio of the area of Δ' to the area of Δ . That is, $RC1 = \frac{A_{\Delta'}}{A_{\Delta}}$. On the other hand, the coverage hole ratio in category 3, RC3, can be stated as the size of coverage hole in of Δ' to its corresponding in Δ . For example, the uncovered area of Δ , denoted by $UNC(\Delta, T(s_i))$, is equal to $A_{\Delta} - ITC(\Delta)$. Thus the ratio is, $RC3 = \frac{UNC(\Delta', T(s_i))}{UNC(\Delta, T^{-1}(s_i))}$. Note that Δ' in $T(s_i)$ and Δ in $T^{-1}(s_i)$ have the same vertices, yet may not be similar in terms of edge length. In both categories 1 and 3, if the ratio is not equal to 1, then there is clearly inaccurate reporting of the sensing coverage of the surroundings of the vertices of Δ (or alternatively Δ'). In this case, the actual coverage in the history is either underestimated or overestimated.

The ratio of perceived coverage hole in category 2 is $RC2 = \frac{UNC(\Delta', T(s_i))}{A_{\Delta'}}$. Similarly, the ratio of actual unreported coverage hole in category 4 is calculated by $RC4 = \frac{UNC(\Delta, T^{-1}(s_i))}{A_{\Delta}}$.

The aforementioned analysis takes in consideration the case where more than one affected objects are neighbours to each other. Assume s_i and s_j are two neighbours and affected objects in $T(s_i)$ (or alternatively in $T(s_j)$). Then $T^{-1}(s_i)$ (or alternatively in $T^{-1}(s_j)$) contains both s_i' and s_j' . Therefore, the effect of anchor misplacement on both s_i and s_j is reflected in all intra-triangle coverage that contains s_i or s_j , or both. However, there will be a redundant calculation of the intra-triangle coverage of the triangle that have both contribution of s_i and s_j as vertices. This redundancy should be considered when calculating the whole intra-triangle coverage in $T(s_i)$ and its history.

C. Proposed Algorithm

The following algorithms identify the different type of coverage holes posed by anchor misplacement and calculate the ratio of each one. Coverage Hole Ratio And Type (*CHRAT*) algorithm assumes that all sensors have been localized, with the existence of anchor misplacement, and their locations are known. *CHRAT* uses the *DAnchD* algorithm in [7] to identify the misplaced anchors. Then finds the set of affected sensors that have been localized by at least one misplaced anchor. For each sensor s_i , *CHRAT* finds the set of collective triangles that have s_i as a common vertex. It finds the set of triangles for each affected sensor s_i for both $T(s_i)$ and its history $T^{-1}(s_i)$ as shown in line 5 and 6. The intersection set of triangles between $T(s_i)$ and its history $T^{-1}(s_i)$ is calculated in line 7. *CHRAT* iterates over all triangles in the intersection and invoke Identify Ratio and Type (*IRAT*) algorithm to identify the coverage hole and determine it ratio.

Algorithm 1: Coverage Hole Ratio and Type (*CHRAT*)

Input: M, N ; //the sets of anchors and sensors, respectively.

Output: *Type_of_coverage_hole, ratio*

```

1  G = Construct_Graph(M); // construct graph G //from
   anchor set only.
2  M' = detect_Misplaced_Anchors(G); //set of misplaced
   anchors
```

```

3  N' = find_Affected_Sensors(M');
4  For each sensor  $s_i \in N'$ 
5      T( $s_i$ ) = findTriangles( $s_i$ );
6      T-1( $s_i$ ) = findTrianglesInHistory( $s_i$ );
7      int_set( $s_i$ ) = T( $s_i$ )  $\cap$  T-1( $s_i$ );
8  End For
9  For each sensor  $\Delta' \in int\_set(s_i)$ 
10      $\Delta$  = historyOfTriangle( $\Delta'$ );
11     invoke IRAT( $\Delta', \Delta, s_i$ );
12 End For
```

IRAT takes a triangle, its history, and its corresponding sensor as inputs. In lines 2 and 6 *HasCoverageHole*(Δ) function checks $\Delta' \in T(s_i)$ and its history $\Delta \in T^{-1}(s_i)$ against the coverage criteria in Lemma 1. This gives four combinations which corresponds to the four categories discussed in Section VI. *current_covered* and *history_covered* are two Boolean variables which indicate whether that the triangles Δ' and Δ , respectively, are covered or not. Once the type of coverage hole, if any, is identified, *IRAT* calculates the ratio of the coverage hole in $T(s_i)$ to the area of coverage hole in $T^{-1}(s_i)$.

Algorithm 2: Identify Ratio and Type (*IRAT*)

Input: triangle Δ , triangle Δ' , affected_sensor s_i

Output: *Type_of_coverage_hole, ratio*

```

1  current_covered = history_covered = true;
2  If HasCoverageHole( $\Delta', T(s_i)$ ) then
3      unc_ $\Delta'$  = UNC( $\Delta', T(s_i)$ );
4      current_covered = false;
5  End if
6  If HasCoverageHole( $\Delta, T^{-1}(s_i)$ ) then
7      unc_ $\Delta$  = UNC( $\Delta, T^{-1}(s_i)$ );
8      history_covered = false;
9  End if
10 If (current_covered && history_covered)
11     Type_of_coverage_hole = Category1;
12     A_ $\Delta'$  = findTriangleArea( $\Delta'$ );
13     A_ $\Delta$  = findTriangleArea( $\Delta$ );
14     ratio =  $\frac{A_{\Delta'}}{A_{\Delta}}$ ;
15     break;
16 End if
17 If (!current_covered && history_covered)
18     Type_of_coverage_hole = Category2;
19     //false perceived coverage hole
20     A_ $\Delta'$  = findArea( $\Delta'$ );
21     ratio =  $\frac{unc_{\Delta'}}{A_{\Delta'}}$ ;
22     break;
23 End if
24 If (!current_covered && !history_covered)
25     Type_of_coverage_hole = Category3;
26     ratio =  $\frac{unc_{\Delta'}}{unc_{\Delta}}$ ;
27     break;
28 End if
29 If (current_covered && !history_covered)
30     Type_of_coverage_hole = Category4;
```

```

31 //unreported actual coverage hole
32  $A_{\Delta} = findArea(\Delta);$ 
33  $ratio = \frac{unc_{\Delta}}{A_{\Delta}};$ 
34 break;
35 End if
36 return Type_of_coverage_hole, ratio;

```

VII. NUMERICAL RESULTS AND DISCUSSION

We use NS-3 to simulate different scenarios of the conducted experiments. The outputs of the simulation step will be inputs for a Visual Studio C++ program which includes our implementation of the proposed algorithm. We also utilize the implementation of a distributed algorithm in [8] to construct the DT. The experiments tend to show the effect of the following parameters: 1) Number of misplaced anchors, 2) Sensing ranges, and 3) The localization error e posed by anchor misplacement. The parameters of all experiments are set as follows, unless otherwise stated. The terrain is divided into four square cells. Each of which is $100 \times 100 \text{ m}^2$. The number of sensor and anchor nodes per cell is 20 and 5, respectively. The transmission range is set to be 142 m. All experiments are conducted under a displacement value of 7m for each misplaced anchor. Furthermore, each misplaced anchors are randomly selected. The average IoT sensing range $r=5\text{m}$ (with variance of 2 m). The results of all conducted experiments are the average of 10 runs. To show the importance of this research, we conduct an experiment that simulates the following real scenario: Given 40 objects in the terrain such as Gas pipes. These pipes are fully covered by sensors to monitor the Gas leakage. Given that an anchor misplacement occurred, we are interested to calculate the proportion of the miss reported objects. In other words, we calculate the percentage of the objects that are not anymore reported by their original sensors. The results are shown in Fig. 7. In the literature, it is widely understood that having more sensors with small sensing ranges provides the best sensing coverage of the terrain. However, our result show that this is not the case when anchor misplacement occurs. It shows using less number of sensors with large sensing range provides better monitoring for the terrain as the percentage of miss reported object decreases by increasing the sensing range. For sensing range 5m, it is required 40 sensors to cover the objects while for larger sensing range fewer sensors are needed.

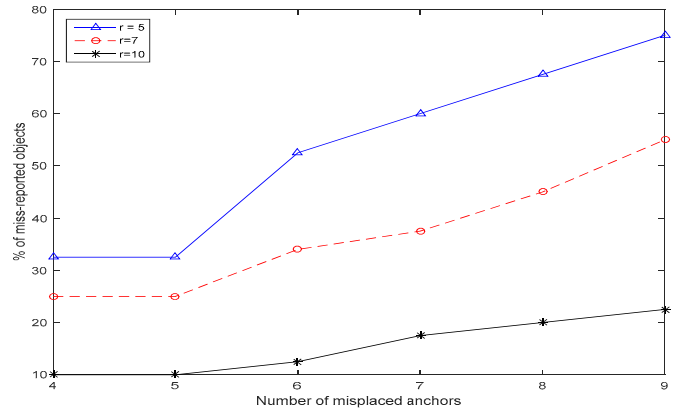


Fig. 7 Number of misplaced anchors vs. percentage of miss-reported objects.

In the second experiment we set the sensing range to 5m (with variance of 2 m) and keep all other parameter settings unchanged. This experiment intends to show the relationship between Root Mean Square Distance (RMSD) of the estimated locations of the sensors, percentage of perceived coverage, and the number of anchors. Perceived coverage of an affected sensor s is the size of the area that is mistakenly reported by s . In other words, it is the part of the sensing disk around s' (i.e. estimated location) that does not intersect with the actual sensing disk of s . We sum up the perceived coverage for all affected sensors and then calculate its percentage to the summation of the actual sensing disks. The results indicates that the percentage of perceived coverage increases proportionally as localization error increases. The results also show that with around half of the anchors are misplaced, around 80% of the reported data is completely inaccurate.

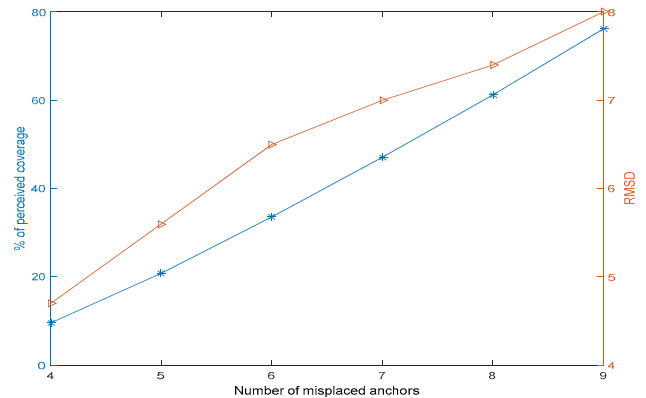


Fig. 8 Number of misplaced anchors vs. perceived coverage and RMSD.

Second interesting evaluation metric is percentage of the area of perceived coverage hole to the area of the covered terrain. We also interested to check on the number of perceived coverage holes posed by anchor misplacement. To evaluate these metrics, we use $100 \times 100 \text{ m}^2$ grid-based deployment to ensure the full sensing coverage with sensing radius sets to 9m. All other parameters are unchanged. The results are shown in Fig. 9. As the number of misplaced anchors increases, the number of coverage holes and their area percentage increase as

well. This is because the more misplaced anchors generate more localization errors and, hence, more perceived coverage holes.

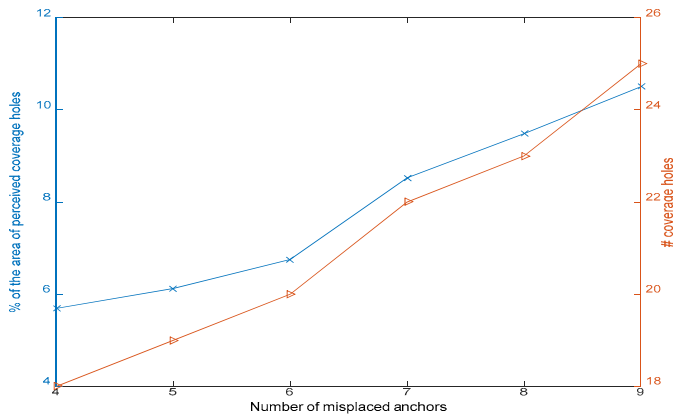


Fig. 9 Number of misplaced anchors vs. the percentage of the area of sensing coverage holes and the number of holes.

These results demonstrate the consistency and the validity of our approach in a typical setting with well-understood sensing coverage parameters.

VIII. CONCLUDING REMARKS

The realization of IoT requires investigating sensing coverage again under the characteristics of IoT itself and according to dynamicity of this environment. This research investigates the IoT sensing coverage problem under that fact that anchor objects are not always declare their correct positions and they could be misplaced easily in the IoT environment. This anchor misplacement leads to new types of coverage hole which degrades the quality of sensing coverage. We consider heterogeneous and non-deterministic deployed IoT objects. Computational geometry provides a tool to provide a localized approach to identify the type of coverage hole and determine its ratio to the total area.

The results show the importance to overcome the anchor misplacement and not to overlook it anymore. The perceived coverage is a serious degradation to the quality of sensing coverage. False sensing reports posed by affected sensing objects may lead to life loss in cases such as wildfire and chemical and gas leakage. While Collective IoT sensors improves the percentage of sensing coverage, anchor misplacement increases the perceived coverage and generate new types of coverage holes. This study also shows that, unlike the common belief, many affected sensors with small sensing range can have an impact on degradation the sensing coverage quality. Our findings suggest that larger sensing range with fewer sensors makes the impact of anchor misplacement less severe. This is also more economic in a very large context such as IoT. These findings can be utilized to tune the sensing range so that keep the impact of anchor misplacement under control. Heterogeneous networks provide cooperative sensing coverage and can expand their lifespan by preserving energy while maintaining the average sensing range at a desired level.

Future work includes providing an approach to mitigate the impact of anchor misplacement on sensing coverage. Study the impact of anchor misplacement of communication coverage is

another urgent research. It is also interesting to investigate what is the threshold values of displacement that do not generate any coverage holes. Another direction is looking into sufficient collective sensing coverage. For example, assume a set of deployed sensors of multiple owners, what is the coverage subset of sensors that provides the best monetary cost with least perceived coverage?.

REFERENCES

- [1] J. Liang, M. Liu, and X. Kui, "A survey of coverage problems in wireless sensor networks," *Sensors & Transducers (1726-5479)*, vol. 163, no. 1, 2014.
- [2] K. Xu, G. Takahara, and H. Hassanein, "On the Robustness of Grid-based Deployment in Wireless Sensor Networks," in *Proceedings of the 2006 International Conference on Wireless Communications and Mobile Computing*, New York, NY, USA, 2006, pp. 1183–1188.
- [3] Y. Al Mtawa, H. Hassanein, and N. Nasser, "Identifying Bounds on Sensing Coverage Holes in IoT Deployments," *IEEE GLOBECOM*, to appear 2015.
- [4] S. M. A. Oteafy and H. S. Hassanein, "Resource Re-use in Wireless Sensor Networks: Realizing a Synergetic Internet of Things," *Journal of Communications*, vol. 7, no. 7, 2012.
- [5] N. Ahmed, S. S. Kanhere, and S. Jha, "The Holes Problem in Wireless Sensor Networks: A Survey," *SIGMOBILE*, vol. 9, no. 2, pp. 4–18, 2005.
- [6] "How big is the Internet of Things and how big will it get?," *The Brookings Institution*. [Online]. Available: <http://www.brookings.edu/blogs/techtank/posts/2015/06/8-future-of-iot-part-1>. [Accessed: 08-Aug-2015].
- [7] Y. Al Mtawa, N. Nasser, and H. Hassanein, "Mitigating Anchor Misplacement Errors in Wireless Sensor Networks," *IEEE International Wireless Communications & Mobile Computing Conference (IWCMC)*, 2015.
- [8] "Delaunay Triangulation Library for C++," 2014. [Online]. Available: <http://www.geom.at/fade2d/html/>. [Accessed: 03-Oct-2014].
- [9] Y. Al Mtawa, "Histories of Iterated Path Graphs," *J. of Combinatorics, Information & System Sciences (JCIS)*, vol. 32, pp. 175–188, 2007.
- [10] Y. Al-Mtawa and M. Jazzer, "On Independence Problem of P2-Graph," *IJCSNS*, vol. 9, no. 1, p. 205, 2009.
- [11] D. M. de Berg, D. M. van Kreveld, P. D. M. Overmars, and D. O. C. Schwarzkopf, "Computational Geometry," in *Computational Geometry*, Springer Berlin Heidelberg, 2000, pp. 1–17.